Electrical Power and Energy Systems 123 (2020) 106238

Contents lists available at ScienceDirect

Electrical Power and Energy Systems

journal homepage: www.elsevier.com/locate/ijepes

A probabilistic method to quantify the capacity value of load transfer

Ilias Sarantakos*, David M. Greenwood, Natalia-Maria Zografou-Barredo, Vahid Vahidinasab, Phil C. Taylor*

School of Engineering, Newcastle University, Newcastle upon Tyne, United Kingdom

ARTICLE INFO

Keywords:
Capacity value
Distribution network
Load transfer
Probabilistic model
Security of supply

ABSTRACT

When a primary substation reaches its capacity limit reinforcement is required, usually via additional circuits. Load transfer constitutes an alternative solution to this problem, as it can provide substantial capacity support at little, or even zero, capital expenditure. This paper provides a probabilistic method which quantifies the capacity value of load transfer using the Effective Load Carrying Capability methodology within a Sequential Monte Carlo Simulation framework. Load transfer is mathematically formulated as a mixed-integer second-order cone programming problem, which can be efficiently solved using commercial solvers. The proposed methodology is applied to a realistically sized distribution network considering three different redundancy levels, namely N-1, N-0.75, and N-0.5. The results show a maximum capacity value of 25% and 37% of the base case demand for manual and remote control load transfer, respectively, for the N-0.5 case with 4.21 MWh/year. The results also show that the capacity value of load transfer is significantly higher if the initial level of reliability of the network is lower, indicating that the network operator is prepared to accept a higher level of risk.

1. Introduction

A key problem in distribution network (DN) planning is to minimize capital investment to meet the growing demand in a reliable way [1]. At the same time, demand is expected to both increase and significantly change shape due to the upcoming electrification of transport and heat [2]. In the past, utilities had a tendency to handle capacity and reliability problems with capital intensive projects, since there was little pressure to reduce expenditure, or no alternative [3]. Today, focus is on deferring network reinforcement through increasing utilization of existing network assets.

Network reinforcement is required when constraint violations exist in a DN, such as voltage and thermal limits, either during normal or N-1 operation. Various assets can be used to provide capacity support, including distributed generation (DG), energy storage systems (ESSs), demand side response (DSR), real-time thermal ratings (RTTR), and load transfer (LT). Various authors have developed methods to quantify the capacity value of these assets [4–7].

One of the main benefits offered by LT is that it can alleviate capacity problems at low (or even zero) capital expenditure levels [3]. The present security of supply standard in the UK (Engineering Recommendation (EREC) P2/7) [8] states that this capacity contribution should be considered when examining the need for reinforcement, but it does not provide a methodology to quantify this value. Hence, investment decisions might be made much earlier than they are actually needed.

1.1. Literature review

Probabilistic methods can be applied to quantify risk and reliability in both transmission and distribution networks. In transmission, papers [9–11] are probabilistic assessments of security of supply, of which [9,10] are based on Monte Carlo Simulation, whereas [11] employs convolution of power plant block availabilities.

In distribution, papers [5,12–14] assess the capacity value of DG and its impact on investment deferral. Pudaruth et al. [13] provide a probabilistic approach to determine the capacity value of DG, using Monte Carlo Simulation to take account of uncertainty. Loss of load probability (LOLP) is used as the reliability index. Dent et al. [14] evaluate the capacity value of DG, using the effective load carrying capability (ELCC) capacity value methodology, and employing the expected power not supplied as the reliability index.

A review of DN security standards in the UK [15] and two papers by Konstantelos et al. [7,16] assess the contribution of ESSs and DSR to security of supply using ELCC, within a Sequential Monte Carlo Simulation (SMCS) framework. Chronological simulation is necessary to capture the effect of time-dependent variables, such as energy constraints, temporal demand characteristics, and state of charge.

* Corresponding authors.
E-mail addresses: ilias.sarantakos@newcastle.ac.uk (I. Sarantakos), phil.taylor@newcastle.ac.uk (P.C. Taylor).

https://doi.org/10.1016/j.ijepes.2020.106238
Received 20 March 2020; Received in revised form 7 May 2020; Accepted 1 June 2020
Available online 18 June 2020

Nomenclature

$A_{k,t}$	Availability of branch k at time t
b_{ij}	Series susceptance in the π-model of branch i-j
D_t	Power of the demand group at time t
$EENS$	Expected energy not supplied
ENS_t	Energy Not Supplied during time period t
g_{ij}	Series conductance in the π-model of branch i-j
I_l, $I_{l,\max}$	Current magnitude/rating of branch l
m, n, N_f	Number of branches/nodes/feeders
$MTTF$	Mean time to failure
$N(i)$	Set of nodes connected to node i by a branch
P_{Ci}, Q_{Ci}	Active/Reactive power curtailment at node i
P_{Di}, Q_{Di}	Active/Reactive power demand at node i
P_{Gi}, Q_{Gi}	Active/Reactive power generation at node i
P_{Ii}, Q_{Ii}	Active/Reactive power injection at node i
R_c	Rating of one incoming circuit
R_{ij}, T_{ij}	Variables associated with branch ij in the conic model
$S_{j,\max}$	Rating of the first branch of feeder F_j at t
S_t^j	Apparent power of the first branch of feeder F_j at t
TTF	Time to failure
TTR	Time to repair
TTS	Time to switch
u_i	Variable associated with node i in the conic model
u_i^l	Variable associated with node i and branch l in the conic model
V_i	Voltage magnitude at node i
V_{max}, V_{min}	Maximum and minimum voltage limit
w_1, w_2	Weights for the objective function terms
X_t	Available capacity of incoming circuits at time t
Y_t	Available contribution of feeders of adjacent substations
Z_t	Loss of load at time t
α_l, α_{ij}	Variable set to 1 if branch $l(ij)$ is closed, 0 if open
β_{ij}	Variable set to 1 if node j is parent of node i, otherwise 0
γ_i	Variable set to 1, if node i is supplied, and to 0 otherwise
θ_i	Voltage angle at node i ($\theta_0 = 0$)
λ	Failure rate
$\Omega_{\text{bus/br}}^{\text{S/S1}}$	Set of buses/branches of substation S/S 1 (under study)
$\Omega_{\text{br}}^{\text{F}_j}$	Set of branches of feeder F_j

Greenwood et al. [6] present a probabilistic method for ESS sizing for a demand peak shaving application and also consider the combination with RTTR to defer conventional reinforcement. References [6,7,15,16] use expected energy not supplied (EENS), as the reliability metric.

So far, limited research has been conducted on the capacity value of LT. Xiao et al. [17] define total supply capability (TSC) as the maximum load that a DN can supply under the N-1 guideline, while satisfying other operational constraints. An optimization-based algorithm – defined as a linear programming problem – is proposed in order to calculate TSC. The TSC concept was extended by Xiao et al. [18] to account for feeder N-1 contingencies (previous methods only considered substation transformer outages). References [19,20] – based on the TSC approach – consider network reconfiguration (load transfer) in their optimization problems. In [19], the reconfiguration capability of the entire DN is investigated to improve TSC through optimal restoration, formulated as a mixed-integer second-order cone programming (MISOCP) problem. Ding et al. [20] consider N-k transformer contingencies, also employing MISOCP, with a decomposition method to solve the formulated two-stage robust TSC model. In [21], a two-stage methodology is presented to improve capacity utilization of substation transformers; the first stage is to optimally reconfigure the substation which will support its failed neighbor, and the second stage is to maximize the LT from the failed to the healthy substation. EREC P2/7 and TSC, which are based on the N-k (most frequently N-1) criterion – a deterministic security standard –, endeavor to define fixed capacity values for stochastic quantities. The approach presented in this paper supports the transition from a deterministic security of supply standard to a probabilistic or reliability-based approach which aims to achieve an acceptable reliability level. Furthermore, this paper addresses network reliability (specifically the fault restoration process) using the SMCS and also considers the energy not supplied (ENS) during failures, in contrast to the aforementioned papers [17–21], which only consider whether or not the load can be supplied (through optimization at a specific instance – usually peak load). These papers also disregard load variation (only [19] considers simplified load profiles) and its associated uncertainty. In order to be able to quantify the capacity value of LT and make decisions about network reinforcement, these factors should be addressed.

1.2. Contribution and organization of the paper

The main contributions of the paper are the following:

(1) Providing a method to quantify the capacity value of load transfer, using a probabilistic and reliability-based analysis. This quantification is implemented using the effective load carrying capability (ELCC) methodology (explained in Section 2.1) within an SMCS framework, which addresses the variation of demand and its inherent uncertainty.
(2) Optimizing the post-fault load transfer by formulating and solving an MISOCP problem (based on [22]). This is a convex optimization problem, which can be efficiently solved to global optimality. The work in this paper advances the state of the art by embedding the MISOCP problem within a probabilistic framework, using the optimality gap to provide a trade-off between accuracy and scalability whilst ensuring this does not unduly decrease network reliability. Furthermore, the objective function is formulated in order to include network losses, which improves LT performance by balancing load between feeders and ensures high quality of the convex relaxation of power flow equations.

The rest of the paper is organized as follows: Section 2 describes the proposed probabilistic method. In Section 3, the case study is presented, and the simulation results are illustrated in Section 4. Section 5 presents a discussion on the findings of this study. Finally, the conclusions are drawn in Section 6.

2. Methodology

In this section, the proposed probabilistic method is described. The aim of the method is to quantify the capacity value of LT based on ELCC. This is achieved using SMCS. The remainder of this section presents: (1) the ELCC capacity value methodology; (2) the SMCS framework; (3) the optimization of LT; (4) optimality gap; and (5) the assumptions made by the authors.

2.1. ELCC-based capacity value

The capacity value of an asset is the additional load that can be accommodated when the asset is employed, while maintaining the same reliability level as when the asset is not present in the network. The capacity value calculation method used in this paper is the effective load carrying capability (ELCC) [23]. This method has been widely employed in the relevant literature [24,25] and – according to Dent et al. [14] – is the most appropriate metric for distribution system planning. Using ELCC as a basis for our method provides confidence and rigour; furthermore, the capacity provided by LT can be meaningfully compared with other conventional and smart network interventions on a level playing field, as illustrated in Section 4.4.

ELCC is a reliability-based method, and therefore requires the selection of a specific reliability index; here EENS has been chosen, as this is the customary index in similar studies in Great Britain [14]. The definition of EENS is as follows:

$$EENS = \sum_{x=1}^{N} p_x \cdot ENS_x \tag{1}$$

where p_x is the probability of a state x, N is the set of states the system could occupy, and ENS_x is the ENS in that state [6]. EENS sums the risk associated with each possible state as a product of its probability and consequence (the energy not supplied), and therefore is more informative than alternative indices, such as LOLP and Loss of Load Expectation which are only a measure of probability, and neglect consequence [26].

First the EENS of the original system (base case) – i.e. without LT – is calculated. Then LT capability is considered which reduces the EENS. The load is then gradually increased, which causes the EENS to increase. When the EENS returns to the level corresponding to the base case, the additional demand that has been accommodated is the ELCC. This is illustrated in Fig. 1. In this paper, ELCC is expressed in terms of percentage load growth.

2.2. EENS calculation within SMCS

ELCC requires a method to evaluate the system reliability in terms of EENS; this is implemented using SMCS [26], because number of states and the time-dependent relationships make analytical approaches impractical. The SMCS stochastically explores the probability states of the system and will return the same answer as the analytical solution with enough iterations. The sequential approach simulates the system lifetime in chronological order for prolonged periods over which statistically representative behaviour will be observed; each time step can be assumed to have an equal probability of occurrence, with different system states as expressed in (1) occurring more or less frequently as dictated by the behaviour of the system. A two-state model (up and down) is employed for the overhead lines (OHLs) and transformers in the network. This method creates an artificial operating history (operation/repair sequence) for each component by randomly sampling up and down times.

The mean time to failure (MTTF) is derived using the failure rate (λ) of an asset as follows:

$$MTTF = \frac{8760}{\lambda} \tag{2}$$

Time to failure (TTF) for each asset is considered exponentially distributed, and failure rate values are taken from [26]. Time to repair (TTR) and time to switch (TTS) are lognormally distributed with mean values taken from [27], and standard deviations equal to one sixth of their mean values [26]. The TTR is assumed to include the time required to restore the network to its original configuration, and that this can be carried out without incurring additional loss of load.

The proposed approach uses a substantial amount of historical data. The demand profile for each simulated day is selected at random from these data; alternatively, the demand profile could be created by a model. For each time period t (considered to be one hour) of this day, the energy not supplied (ENS_t) is determined as explained below. An overview of the proposed method is provided in Fig. 2. To summarize, the uncertainties in the SMCS include:

(1) Time to failure – exponentially distributed.
(2) Time to repair – lognormally distributed.
(3) Time to switch – lognormally distributed.
(4) Demand – randomly selected from historical data.

The demand group D_t is supplied by two incoming circuits, which have available capacity X_t. The supply to the primary substation is assumed to be totally reliable. We also consider the available contribution from the neighboring substations, Y_t. All the aforementioned variables are random, and we are interested in the loss of load (Z_t) and the ENS_t.

The available capacity of the incoming circuits (X_t) can take the values 0, R_c, and $2R_c$, depending on the availability of each circuit. This can be written as follows:

$$X_t = \begin{cases} 0, & \text{no circuits available} \\ R_c, & \text{one circuit available} \\ 2R_c, & \text{two circuits available} \end{cases} \tag{3}$$

When both incoming circuits are available, the loss of load will be zero and the network will remain in its initial configuration. If the network was in a different configuration in the previous time step, then it is set back to its original configuration. The loss of load is also zero if there is: (i) an outage of an incoming circuit, (ii) demand is lower than the available incoming circuit capacity, and (iii) the network has not been reconfigured.

LT takes place if there is an outage on at least one of the incoming circuits, and the demand cannot be met by the remaining capacity. The LT is completed once the switching actions (in the primary DN) have been performed. The time required to complete this is the switching time. During this time period, $Y_t = 0$, and therefore D_t can be supplied only by X_t. The loss of load in this case will be:

$$Z_t = D_t - X_t \tag{4}$$

and the ENS_t will be equal to:

$$ENS_t = \max(Z_t \cdot \Delta t, 0) \tag{5}$$

In the reconfigured network, a subset of the demand ($D_{1,t}$) continues to be supplied by the substation under study, while the second subset ($D_{2,t}$) is transferred onto the feeders of different substations through normally open points (NOPs). This can be expressed as:

$$D_t = D_{1,t} + D_{2,t} \tag{6}$$

The network configuration remains fixed until the failed incoming circuit has been repaired. During this time, the first subset of the demand ($D_{1,t}$) can be supplied only by the available capacity of the substation (X_t). Hence, the loss of load and the ENS for $D_{1,t}$ are derived as

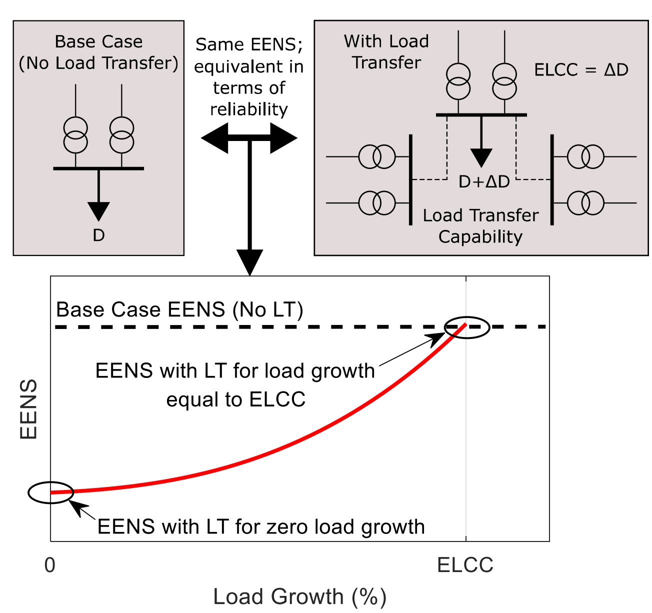

Fig. 1. The main concept of the ELCC methodology for load transfer.

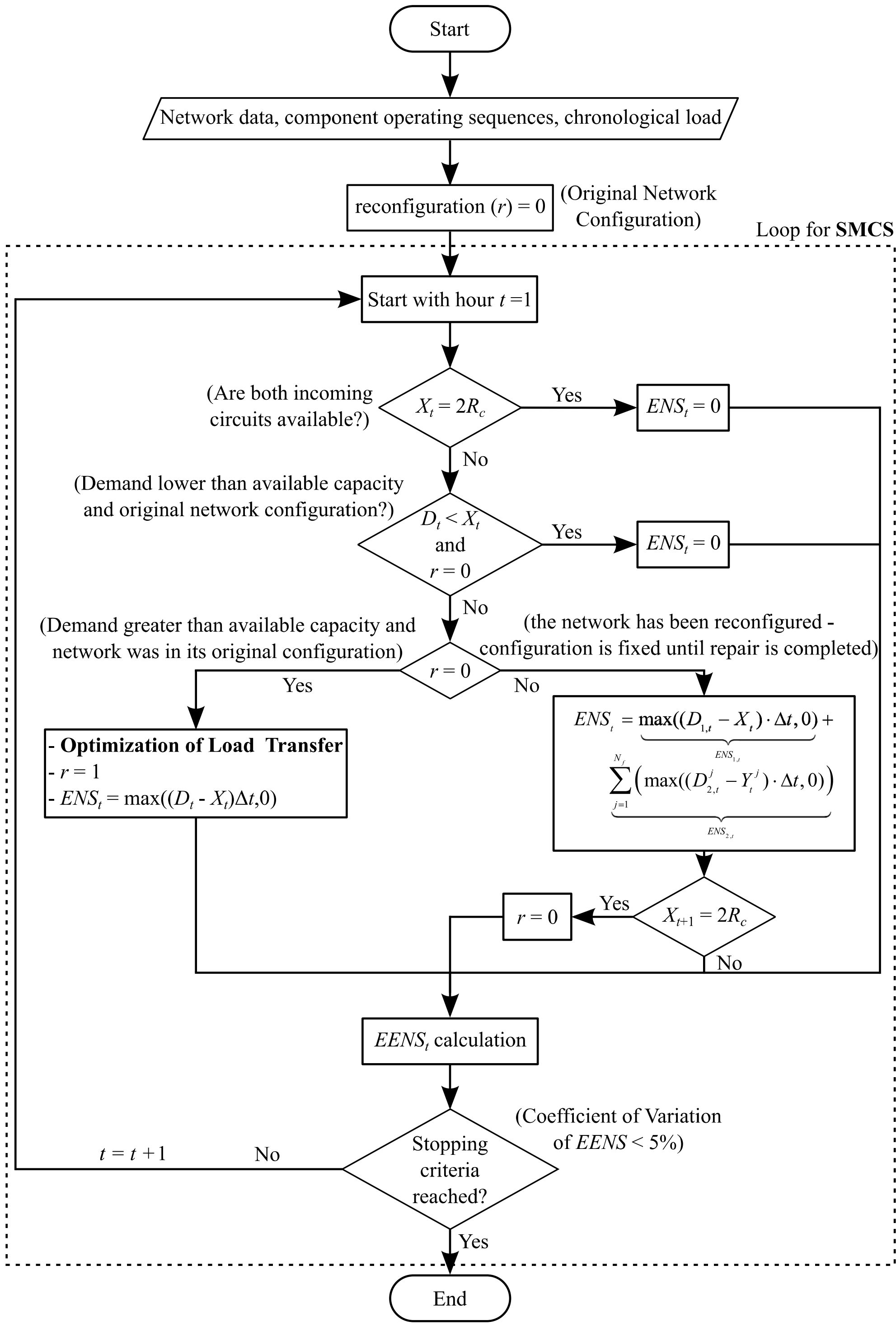

Fig. 2. Overview of the proposed method. Variable r in the flowchart is zero, if the network has not been reconfigured (i.e. the network is in its original state), whereas $r = 1$, if the network has been reconfigured (to perform load transfer) and has not returned to its initial state yet.

follows:

$$Z_{1,t} = D_{1,t} - X_t \tag{7}$$

$$ENS_{1,t} = \max(Z_{1,t}\cdot\Delta t,\ 0) \tag{8}$$

The second subset of the demand group ($D_{2,t}$) is equal to the sum of each demand $D_{2,t}^j$ (determined by the optimization problem formulated below) that is transferred from feeder F_i (of the considered substation) to an adjacent feeder F_j (of a different substation), i.e.

$$D_{2,t} = \sum_{j=1}^{N_f} D_{2,t}^j \tag{9}$$

where $D_{2,t}^j$is the load transferred from feeder F_i to an adjacent feeder F_j via a NOP, at time t.

Each $D_{2,t}^j$ (during the repair process) can be supplied only by the available contribution of the adjacent feeder F_j (Y_t^j), which can be defined as:

$$Y_t^j = \max((S_{j,\max} - S_t^j), 0)\cdot \prod_{k\in\Omega_{\mathrm{br}}^{\mathrm{F}j}} A_{k,t} \tag{10}$$

Eq. (10) expresses the available capacity margin of feeder F_j; $A_{k,t}$ refers to the availability of the branches of feeder F_j.

In this case, the loss of load and the ENS are:

$$Z_{2,t}^j = D_{2,t}^j - Y_t^j \tag{11}$$

$$ENS_{2,t} = \sum_{j=1}^{N_f} (\max(Z_{2,t}^j\cdot\Delta t, 0)) \tag{12}$$

The total hourly ENS (after having reconfigured the network and until the repair at the substation has been completed) is then obtained by:

$$ENS_t = ENS_{1,t} + ENS_{2,t} \tag{13}$$

Once the repair has been completed, the network is set to its initial configuration, in which it remains until another failure occurs. Then, using *ENS* from simulated hour 1 to *t*, the $EENS_t$ (per calendar year) is derived as follows:

$$EENS_t = \frac{8760}{t}\cdot \sum_{t'=1}^{t} ENS_{t'} \tag{14}$$

Eq. (14) assumes each hour has the same probability of occurrence. The coefficient of variation (CoV) of the EENS is calculated every 100 simulated years to decrease the number of computations. The number of simulated days is not fixed; the convergence criterion (CoV) determines how many days will be simulated, and it takes hundreds of thousands, or even millions, of simulated days for the SMCS to be completed.

$$CoV_{EENS,t} = \frac{\mathrm{std}(EENS(1{:}\,t))}{\mathrm{mean}(EENS(1{:}\,t))} \tag{15}$$

where $CoV_{EENS,t}$ is the coefficient of variation of the EENS at time step *t*; std(*EENS*(1:*t*)) is the standard deviation of the $EENS_t$ values from 1 to *t*; and mean(*EENS*(1:*t*)) is the average of the $EENS_t$ values from 1 to *t*.

When CoV falls below 5% [28], the SMCS is terminated, and the *EENS* for this simulation equals $EENS_t$. The EENS is calculated for each season separately because of seasonal variations in the demand and line ratings; the final EENS is the weighted sum of the previous results [29], which combines statistically representative results for each season to give a statistically representative result for a year.

$$EENS = \frac{3}{12}EENS_{win} + \frac{2}{12}EENS_{spr} + \frac{4}{12}EENS_{sum} + \frac{3}{12}EENS_{aut} \tag{16}$$

2.3. Optimization of load transfer

Determining which loads to transfer from the faulted to the healthy substation is not trivial and transferring the wrong loads could lead to an unnecessarily low level of reliability. The selection of which loads to transfer from the failed substation to the healthy one through the feeder NOPs has been formulated as an MISOCP problem based on [22].

The objective function (15) comprises two terms: the first is the power not supplied to load points of the substation under consideration, and the second is network losses. Minimization of losses (which leads to load balance between feeders) is incorporated to restrict the amount of load transferred to neighboring substations. Without the use of network losses in the objective function, more load points than strictly necessary would be transferred to adjacent feeders; if the load on those feeders increased in subsequent time steps, the adjacent feeders would be overloaded, and some customers would have to be taken off supply.

There is also another reason why losses are used in the objective function. According to [22], minimizing losses (which is equivalent to minimizing the sum of net real power injections at all nodes (17)), increases the values of R_{ij} because $g_{ij} > 0$ in (30). This results in the rotated conic quadratic constraints in (34) being binding at optimality [30]. Consequently, the incorporation of losses (or an equivalent function that would increase the values of R_{ij}) ensures the high quality of the convex relaxation (of power flow equations).

$$\text{minimize } w_1 \sum_{i\in\Omega_{\mathrm{bus}}^{\mathrm{S/S1}}} P_{Ci} + w_2 \sum_{i=0}^{n} P_{Ii} \text{ subject to} \tag{17}$$

The MISOCP formulation requires the definition of the following new variables [30]:

$$u_i = \frac{V_i^2}{\sqrt{2}},\ \ i = 1, \ldots, n \tag{18}$$

$$R_{ij} = V_i V_j \cos(\theta_i - \theta_j),\ \ ij \in \text{set of lines } l = 1, \ldots, m \tag{19}$$

$$T_{ij} = V_i V_j \sin(\theta_i - \theta_j),\ \ ij \in \text{set of lines } l = 1, \ldots, m \tag{20}$$

The constraints of the problem ((21)–(40)) are presented below. A detailed explanation of constraints (21)–(34) can be found in [22]. The equations that ensure the radiality of the network are based on the following feature of the spanning tree: every node (except the substation node) has exactly one parent.

(1) Network radiality constraints

$$\beta_{ij} + \beta_{ji} = \alpha_l,\ \ l = 1, \ldots, m \tag{21}$$

$$\sum_{j\in N(i)} \beta_{ij} = 1,\ \ i = 1, \ldots, n \tag{22}$$

$$\beta_{0j} = 0,\ \ j \in N(0) \tag{23}$$

where index 0 corresponds to the substation node.

$$\beta_{ij} \in \{0, 1\},\ \ i = 1, \ldots, n,\ \ j \in N(i) \tag{24}$$

$$0 \leqslant \alpha_l \leqslant 1,\ \ l = 1, \ldots, m \tag{25}$$

Eq. (21) shows that a branch *l* is in the spanning tree, if either node *j* is the parent of node *i* ($\beta_{ij} = 1$), or node *i* is the parent of node *j* ($\beta_{ji} = 1$). Every node (except the substation node) is required to have exactly one parent (22); equation (23) indicates that the substation node has no parents.

(2) Branch connection status constraints (for $l = 1,\ldots,m$)

$$0 \leqslant u_i^l \leqslant \frac{V_{i,\max}^2}{\sqrt{2}} a_l \tag{26}$$

$$0 \leqslant u_j^l \leqslant \frac{V_{j,\max}^2}{\sqrt{2}} a_l \tag{27}$$

$$0 \leqslant u_i - u_i^l \leqslant \frac{V_{i,\max}^2}{\sqrt{2}} (1 - a_l) \tag{28}$$

$$0 \leqslant u_j - u_j^l \leqslant \frac{V_{j,\max}^2}{\sqrt{2}} (1 - a_l) \tag{29}$$

where u_i^l and u_j^l are defined for each branch *l* (*ij*), and are set to zero, if the branch is disconnected ($\alpha_l = 0$) and take the values u_i and u_j, if the branch is connected ($\alpha_l = 1$).

(3) Real and reactive power injection constraints ($i = 1,\ldots,n$)

$$P_{Ii} = \sum_{j\in N(i)} (\sqrt{2} g_{ij} u_i^l - g_{ij} R_{ij} - b_{ij} T_{ij}) = P_{Gi} - P_{Di} + P_{Ci} \tag{30}$$

$$Q_{Ii} = \sum_{j\in N(i)} (-\sqrt{2} b_{ij} u_i^l + b_{ij} R_{ij} - g_{ij} T_{ij}) = Q_{Gi} - Q_{Di} + Q_{Ci} \tag{31}$$

(4) Voltage magnitude limits ($i = 1,\ldots,n$)

Table 1
Sensitivity analysis for the selection of the objective function weights.

w_1	≤1.0	1.5	2.5	4.0	10	20	100
w_2	Fixed at 1.0						
Comp. Time (s)	More disconnection than required	66	25	57	55	45	46

$$\frac{V_{i,\min}^2}{\sqrt{2}} \leqslant u_i \leqslant \frac{V_{i,\max}^2}{\sqrt{2}} \tag{32}$$

(5) Maximum branch current limits ($l = 1,\ldots,m$)

$$I_l^2 = \sqrt{2}\,(g_{ij}^2 + b_{ij}^2)(u_i^l + u_j^l - \sqrt{2}R_{ij}) \leqslant I_{l,\max}^2 \tag{33}$$

Eq. (33) expresses squared branch current as a linear equation, given that the shunt susceptance (in the π-model) of branch ij is zero.

(6) Rotated conic quadratic constraints [22,30]

$$2u_i^l u_j^l \geqslant R_{ij}^2 + T_{ij}^2,\ \ R_{ij} \geqslant 0,\ \ ij \in \text{set of lines } l = 1,\ldots,m \tag{34}$$

(7) Power curtailment constraints ((35)–(38) based on [21])

$$P_{Ci} = Q_{Ci} = 0,\ \ i \notin \Omega_{\text{bus}}^{\text{S/S1}} \tag{35}$$

Eq. (35) state that no load curtailment is performed at assisting substations.

$$P_{Ci} = P_{Di}(1 - \gamma_i),\ \ i \in \Omega_{\text{bus}}^{\text{S/S1}} \tag{36}$$

According to (36), each LP of the substation under consideration is either fully supplied or not supplied at all.

$$P_{Ci} \leqslant P_{Di}(2 - \beta_{ji} - \gamma_j),\ \ i \in \Omega_{\text{bus}}^{\text{S/S1}},\ \ j \in N(i) \tag{37}$$

Eq. (37) declares that if the load point at node j is fully supplied ($\gamma_j = 1$), and node i is the parent of node j ($\beta_{ji} = 1$), the load point at node i should also be fully supplied ($P_{Ci} = 0$).

$$Q_{Ci} = P_{Ci}\frac{Q_{Di}}{P_{Di}},\ \ i \in \Omega_{\text{bus}}^{\text{S/S1}},\ \ P_{Di} \neq 0 \tag{38}$$

Eq. (38) indicates that active and reactive power curtailments are proportional to each other. To avoid an open branch between any two fully curtailed LPs, and also to restrict any load curtailment only to the considered substation (at the time when LT is required), we also add the following constraint (39):

$$a_{ij} \geqslant 1 - \gamma_j,\ \ j \in \Omega_{\text{bus}}^{\text{S/S1}} \tag{39}$$

(8) Assisting substation constraint

Finally, to avoid transferring load to the failed substation, the branches of the assisting substations are assumed to be closed.

$$\alpha_l = 1,\ \ l \notin \Omega_{\text{br}}^{\text{S/S1}} \tag{40}$$

The formulated model (objective function (17) subject to constraints (21)–(40)) is an MISOCP problem, which means that an optimal solution can be found using commercially available solvers such as Gurobi, MOSEK, and CPLEX [31–33]. The network configuration is defined by the values of a_l, which represent the status (connected/disconnected) of each branch l. Using this information, we can determine the LT to the assisting substations ($D_{2,t}$), as well as the remaining subset of the load at the failed substation ($D_{1,t}$). These values are then used to calculate the energy not supplied, as described earlier.

In the case of a double circuit outage ($X_t = 0$), the optimal reconfiguration is the maximum LT from the failed substation to the assisting ones – assisting substations take up all load points from the failed substation, if possible. This can be achieved by the first term of the objective function, without the need to add the second term of network losses. However, in the case of a single circuit outage ($X_t = R_c$), which is much more frequent, the LT should be slightly higher than the demand that cannot be met by the remaining incoming circuit capacity. Without the use of the second term, more load points than necessary would be transferred to assisting substations. This could increase ENS because feeders that take up the additional demand might be overloaded as load varies with time.

A weight value of 2.5 has been chosen for the first term of the objective function, because it should be prioritized over the second term, for which a value of 1.0 has been selected. The weight of the first term should not be too small – compared to the weight of the second term – as this would cause the disconnection of load points in order to reduce losses. The weight values above were chosen based on a sensitivity analysis, the results of which are illustrated in Table 1. Because we are interested in the ratio between the power not served and active power losses, w_2 was fixed at a value of 1.0, and a range of values were investigated for w_1. Value ≤ 1.0 for w_1 caused a disconnection of additional demand to reduce losses, and therefore was unacceptable. When $w_1 \geq 1.5$, we obtain the minimum disconnection, and consequently, all these values are acceptable. However, the optimization time varies; we select the value for w_1 which corresponds to the lowest average computational time. This sensitivity analysis was carried out solving the model to optimality across five loading levels (18.94–23.15 MVA) considering one incoming circuit outage.

Fig. 3 illustrates the proposed method in three cases. In Fig. 3(a), the available capacity of the incoming circuits is sufficient to supply the demand, despite the circuit outage, and therefore no LT is required; the ENS is zero. In (b), at 17:00, the demand exceeds the available capacity X_t, which leads to loss of load until the failed circuit has been repaired (20:00); this case considers that there is no LT capability. In contrast, (c) assumes that LT can be performed, which can significantly reduce the ENS. However, the LT cannot be implemented until switching operations have been completed, which results in a low – but unavoidable – level of ENS.

2.4. Optimality gap

The proposed model might require a computational time of several days if the optimization of LT is solved to global optimality on a complex network, given that this optimization is incorporated in an SMCS and the optimization problem must therefore be solved thousands of times. The optimality gap can be relaxed to substantially reduce the computational time whilst ensuring high-quality solutions. Relaxing the optimality gap enables the solver to return a solution which is within a specified distance of the global optimal solution much more quickly than converging to full optimality.

Mixed-integer programming (MIP) problems are generally solved using a branch-and-bound (B&B) algorithm [34]. In MIP, a significant parameter is the relative optimality gap tolerance (MIPGap) below which the optimizer terminates. The MIPGap is defined as follows [31]:

$$MIPGap = \frac{|ObjBound - ObjVal|}{|ObjVal|} \tag{41}$$

where *ObjBound* and *ObjVal* are the MIP objective bound and incumbent, respectively. The incumbent is the best integer feasible solution that has been found at any point in the search tree of B&B. The best objective bound is equal to the minimum of the optimal objective values (of relaxed MIPs) of all of the current leaf nodes [34]. A MIPGap of 10% denotes that the *maximum* distance to optimality is 10% – actual distance can be (much) lower. For example, if the optimizer – at some point in its search procedure – obtains a value of 0.5 for the incumbent and 0.46 for the objective bound, then it will stop, as the MIPGap at that point is 8%. The first obtained gap below the tolerance might be lower than that, as shown in Section 4.2, which means that actual distance to optimality can be significantly smaller than the specified

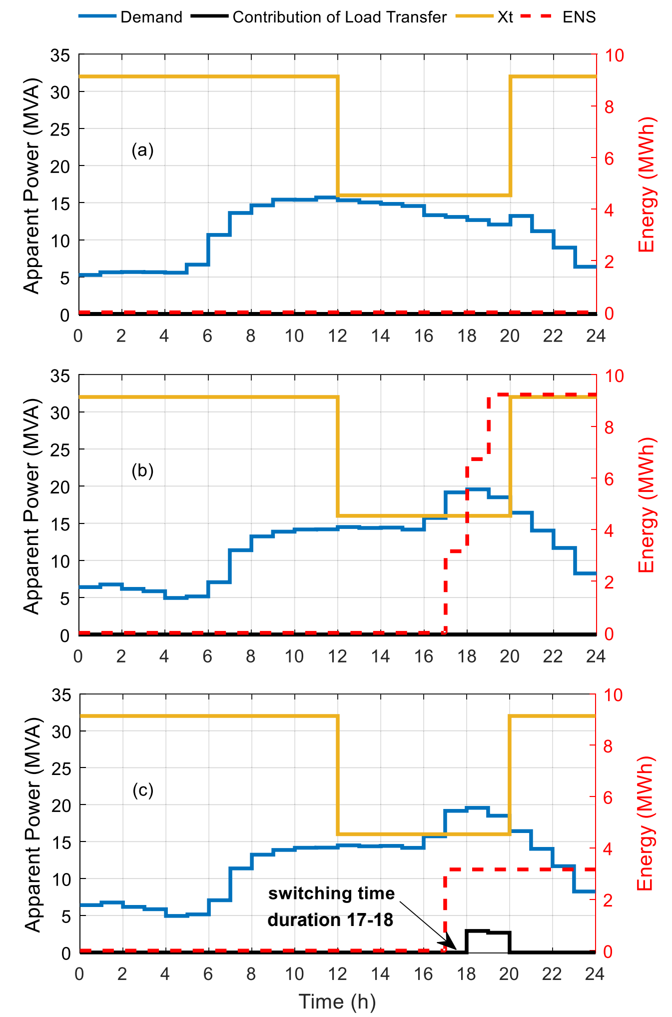

Fig. 3. Illustrative scenarios to clarify the proposed method. In (a) the demand is lower than the available incoming circuit capacity (X_t), and therefore there is no need for reconfiguration; in (b) the demand exceeds the available capacity, resulting in loss of load, since there is no reconfiguration capability; and (c) illustrates the same case as (b), but with reconfiguration capability, which leads to an improved level of ENS. The duration of the switching time in (c) is one hour – from 17:00 to 18:00.

MIPGap.

2.5. Assumptions

(1) This paper considers manual and remote control LT. This is considered in the model by modifying the value of the switching time. In the case of remote control LT, all switches are assumed to be remote controlled switches (RCSs).
(2) This paper is carried out from the perspective of the 33 kV network and therefore focuses on failures occurring in the incoming circuits. EENS arising from failures in the primary DN is therefore not considered, but these failures are included when assessing the available contribution of the interconnecting feeders to the adjacent substation (i.e. for the alternative supply of the load points of the considered substation).
(3) The network configuration, after the switching actions have been performed (during the switching time), remains fixed until the repair of the failed component has been completed; then the network is set to its original configuration as part of the repair. We assume that the time to restore the network to its original configuration is included in the repair time and that it can be completed without incurring additional energy not supplied.
(4) The optimization of the LT is carried out when there is demand which cannot be met by the available incoming circuit capacity. The aim is the minimization of power not supplied at that time step. For the subsequent time steps (and until the failed component has been repaired), the power not supplied is calculated by the differences of the available circuit capacities and the corresponding loads. This is a conservative assumption because in some cases additional switching could be conducted to mitigate further energy not supplied, although the objective function used does ensure some headroom to accommodate demand increases at both the failed and supporting substation.
(5) Load curtailment variables are not used to model demand response; they are rather used to model the power not supplied when reconfiguring the network.

3. Case study

3.1. Test network

The test network is a real-world DN operated by Taiwan Power Company (TPC) [35] and is presented in Fig. 4. This network has been extensively used in the relevant literature (e.g. [20,22]). It is an 11.4 kV network with 11 feeders, 83 normally closed branches, and 13 normally open branches. The customer types for each load point were taken from [36]. The circuits (transformers and OHLs), which supply the network are shown in Fig. 5. The substation voltage is set at 1.06 pu (maximum limit), and the minimum allowed voltage is 0.94 pu (UK medium voltage distribution limits have been considered [37]). The feeder 65 °C thermal limits (for each season) are given in Table 2 [38].

3.2. Electricity demand data

Real demand data for six years are taken from a 33/11 kV substation from the UK Power Networks' Smarter Network Storage project [39] and are adjusted appropriately to match the demand of S/S 1 of the case study network. The substation demand data are disaggregated into load point demands according to two coefficients: (1) a time-varying one, which expresses the share of the load type of the load point in the total substation demand at time t; and (2) a time-invariant one, which expresses the share of the load point in the total demand of this type. This method is described in detail in [40].

To demonstrate the significance of the base case reliability, three different cases – which correspond to redundancy levels of N-1, N-0.75, and N-0.5 (as in [16]) – are considered:

(1) N-1: Peak demand must be supplied in the case of one circuit outage. This corresponds to a peak demand of 16 MVA (in the winter), which is equal to the N-1 transformer capacity. This case represents a network fully compliant with the N-1 reliability criterion.
(2) N-0.75: Peak demand can exceed the incoming capacity by up to 25% during a single circuit outage (equivalent to an "outage" of 0.75 circuits), which corresponds to a peak demand of 20 MVA.
(3) N-0.5: Peak demand can exceed the incoming capacity by up to 50% during a single circuit outage (equivalent to an "outage" of 0.5 circuits), which corresponds to a peak demand of 24 MVA.

In other words, for two 10 MVA circuits, the peak demand at N-1 would be 10 MVA, at N-0.75 would be 12.5 MVA, and at N-0.5 would be 15 MVA. Networks with redundancy levels less than N-1 (e.g. N-0.75 and N-0.5) are increasingly of interest to researchers and network operators since they can deliver better value for customers while maintaining high reliability through smart interventions [16].

Fig. 6 shows the cumulative probability of various levels of substation loading at each hourly interval during a day in winter for each

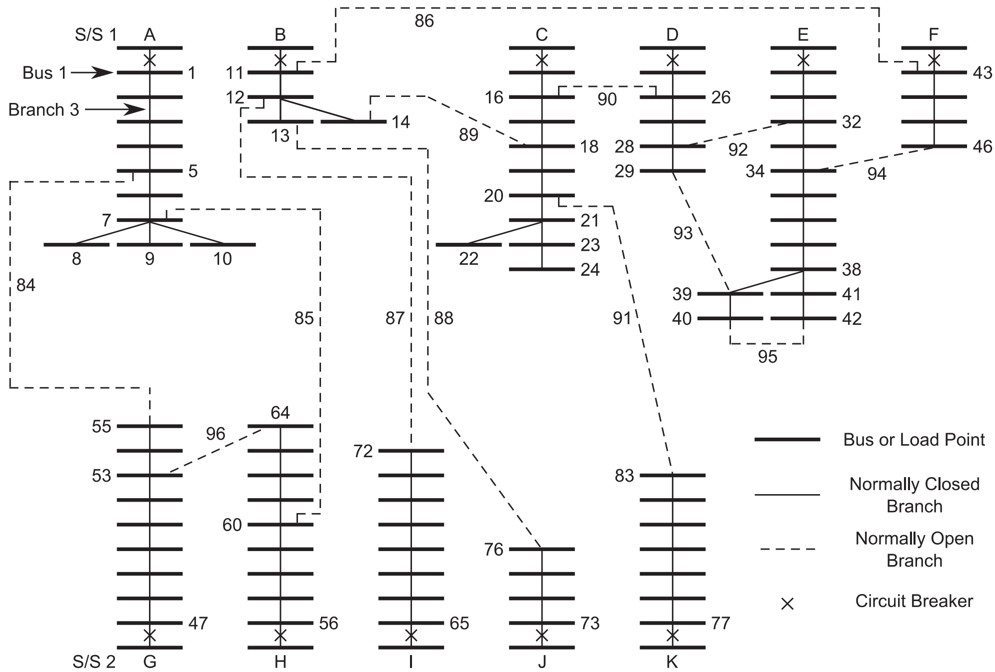

Fig. 4. The Taiwan Power Company Distribution Network. Substation S/S 1 supplies feeders A, B, C, D, E, and F; substation S/S 2 supplies feeders G, H, I, J, and K.

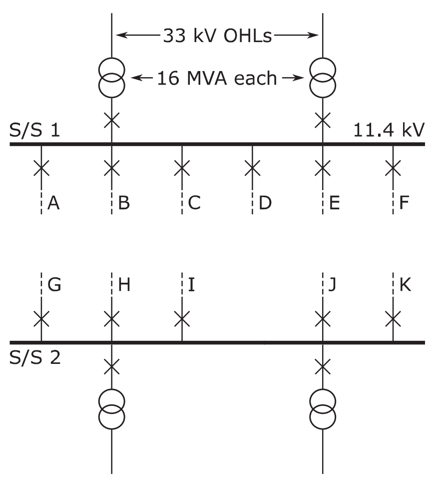

Fig. 5. The upstream network circuits that supply the Taiwan Power Company Distribution Network.

Table 2
Feeder Thermal Limits.

Season	65 °C Limit (MVA)
Winter	12.55
Spring/Autumn	11.79
Summer	10.65

redundancy level.

3.3. Reliability data

The substation under study (S/S 1) consists of two transformers, and is assumed to be supplied by two 11 km 33 kV OHLs. The reliability data for the aforementioned assets, as well as for 11.4 kV OHLs (in primary DN), are presented in Table 3 (according to [27]). Switching time is considered 1 h for manual switches [27] and 15 min for RCSs [41].

3.4. Implementation

The methodology developed in Section 2 was applied to the test network shown in Fig. 4 using the input data described in Section 3. The proposed model has been built in MATLAB R2017a; the MISOCP model was optimized using Gurobi [31]. An Intel Core i7 octa-core processor at 3.0 GHz with 32 GB of RAM was used for the simulations. The base case corresponds to: (1) no LT capability; and (2) zero load growth.

4. Results

4.1. ELCC Results: Manual and remote control LT

Fig. 7 shows the EENS for manual and remote control LT for various levels of load growth for N-1, N-0.75, and N-0.5 redundancy levels. The base case reliability in the N-1 case is 17 kWh/year; this value is so low because it corresponds to the energy not supplied during double circuit outages, since the demand can always be supplied in the case of a single circuit outage. EENS reaches the base case value for a load growth of 7% and 16% for manual and remote control LT, respectively; therefore the corresponding ELCCs are 7% and 16% of the base case demand. The capacity value is higher for remote control switching because the unavoidable ENS which occurs during switching – as illustrated in Fig. 3 – is significantly (around 75%) lower because the switching time has reduced from 60 min to 15 min. Consequently, a greater increase in loading will be required to return the EENS to the base case level. In a similar way, the capacity values for the N-0.75 and N-0.5 cases are 14%/25% and 25%/37% of the base case demand, respectively, with the first percentage corresponding to manual LT and the second to remote control LT.

Fig. 8 illustrates the ELCC-based capacity value of manual and remote control LT along with the associated EENS for the three considered redundancy levels. This figure demonstrates that the capacity value is significantly influenced by the considered redundancy. The less the required redundancy, the higher the value of the EENS index; and the higher the acceptable EENS, the higher the contribution LT can make.

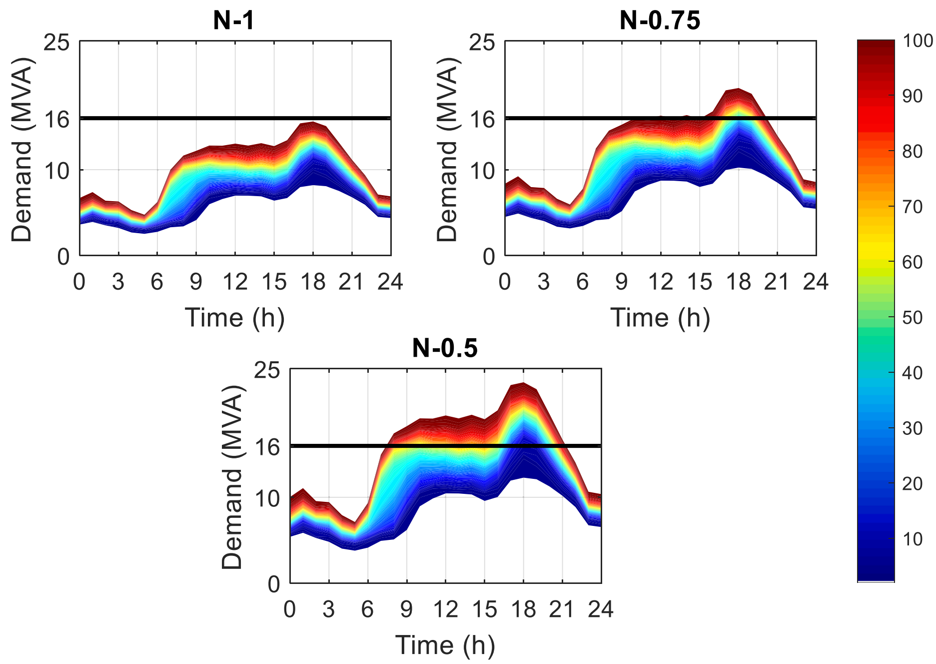

Fig. 6. Demand quantiles for winter for each redundancy level. The colour bar indicates the cumulative probability of each loading level with the corresponding colour. The black line indicates the single transformer capacity.

Table 3
Reliability Data.

Asset	Failure Rate (λ)	Repair Time
Transformer	0.015f/y	15 h
33 kV OHL	0.046f/y·km	8 h
11.4 kV OHL	0.065f/y·km	5 h

4.2. Computational performance

Locating the optimal solution for the TPC DN takes approximately 25 s. Taking into account that the SMCS requires thousands of optimization runs for each simulation, the computational time can be in the order of days, unless a more powerful processor is used. Relaxing the MIPGap – as suggested in [22] – provides an attractive alternative, as setting the MIPGap to 10%, yields an average optimality gap of 2.3% and an average computational time for each optimization run of 1.2 s. The average simulation time for the results (considering LT) presented above is approximately 5 h. Each simulation can be run separately, and the optimizer can exploit the parallel computing capability of a CPU, if available.

4.3. Comparison with the TSC method

This section compares the proposed approach with the TSC method presented in [19]. TSC is an alternative method for evaluating the maximum loading capacity of a DN; it is based on a deterministic criterion and determines whether the load can be supplied during an N-1 transformer contingency. The associated reliability level is not evaluated. If a reliability-based approach is employed, then the N-1 criterion is not required, and a comparison can be made with an acceptable reliability level set by the distribution network operator (DNO) or the regulator.

TSC calculates the maximum load that can be accommodated during an N-1 transformer contingency before any operational constraints are violated. This means that TSC does not allow a demand greater than the N-1 transformer capacity (16 MVA here). For this reason, the comparison of TSC with the proposed approach is performed using the N-1 case in Section 4.1.

The TSC method in [19] indicates an acceptable load growth of 52%. Because TSC does not assess the associated reliability level, we have calculated this value (in terms of EENS) considering both manual and remote control LT; the corresponding EENS are 855 and 386 kWh/year, respectively. These values are much higher (50 and 23 times) than that of the base case. Furthermore, the TSC method cannot capture the level of automation in switching actions and thus produces a single capacity value regardless of the degree of automation. The results are presented in Table 4.

Although it is difficult to make a direct comparison between the method described by this paper and TSC, the value in doing so is to demonstrate the potential cost of making decisions blind to reliability. TSC will remain the same regardless of the switching times, repair times, and failure rates within the network, while our method will alter the network's load carrying capability based on the impact these parameters have on network reliability.

4.4. Comparison with energy storage

This section provides a comparison between the ELCC-based capacity value of LT and Energy Storage Systems (ESSs). Using results from [16] and ESS cost data from [42], we obtain the results presented in Table 5. The ESS, in both studies, is connected at the low voltage busbar of the primary substation (here S/S 1). As shown in Table 5, the greatest capacity support per 1 M€ corresponds to the 2 MW/4 MWh ESS at N-1 redundancy level, which is equal to 1.36% load growth/M€. Manual LT has zero cost because it already exists and provides a capacity contribution of 7%; remote control LT (for the whole network) would cost an estimated 1.42 M€ and yields a capacity support equal to 16%. The switch upgrade cost is calculated, based on [43], assuming an upgrade cost of €17,100 for each switch and 83 switches in the network. Consequently, load transfer capability is a valuable solution for capacity support provision, as it already exists in the majority of the networks, and can provide significant contribution to security of supply at zero (for manual LT) or relatively low cost (compared to a capital-intensive investment of an ESS). However, if an ESS it to be commissioned, it will be used to provide additional services (e.g. frequency response [44], arbitrage) as well, which might justify the investment.

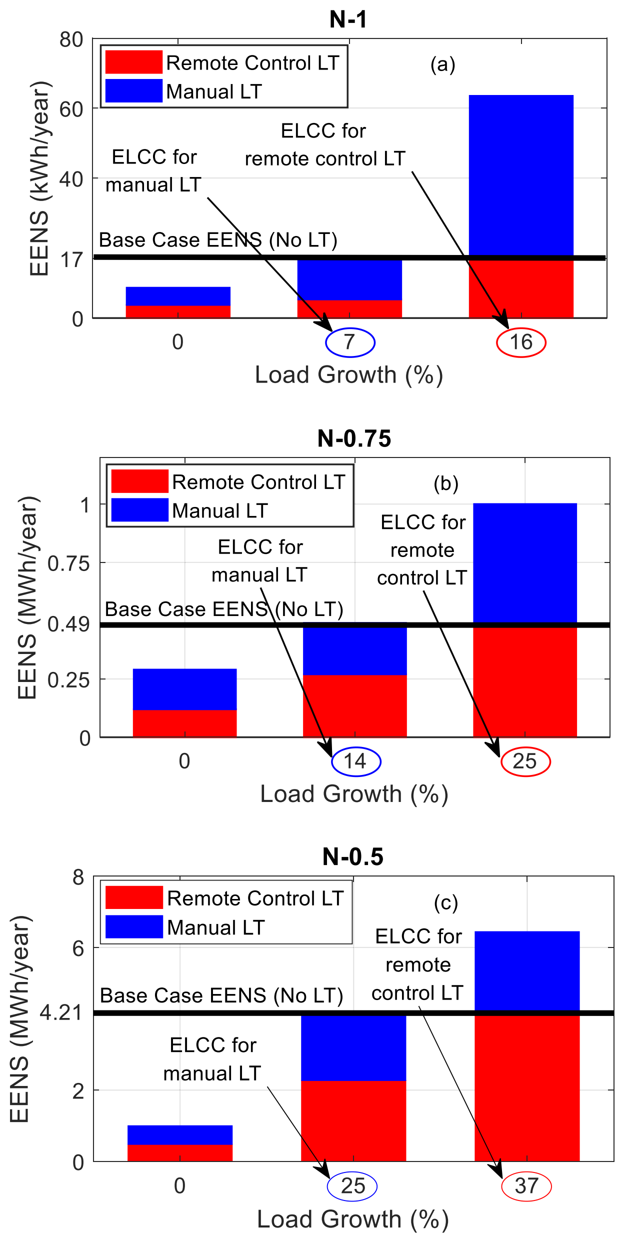

Fig. 7. EENS for manual and remote control LT at three levels of load growth for N-1 (a), N-0.75 (b), and N-0.5 (c) redundancy levels; when EENS reaches the base case value, this load growth constitutes the ELCC-based capacity value.

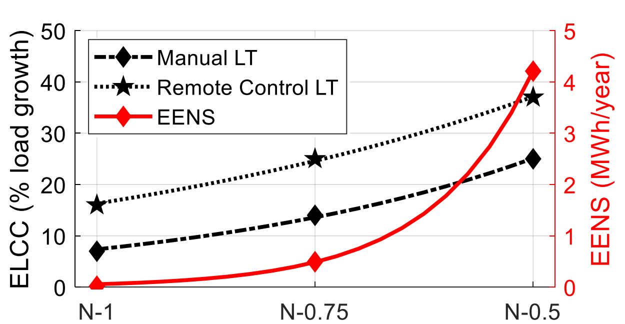

Fig. 8. ELCC and EENS for all three base cases, which correspond to three different redundancy levels. The ELCC is significantly influenced by the considered redundancy.

Table 4
Comparison with TSC.

Method	ELCC/TSC	EENS (kWh/year)
N-1 Case (No LT) – Section 4.1	–	17
Proposed Approach (Manual LT)	7%	17
Proposed Approach (Remote Control LT)	16%	17
TSC [11] (not reliability-based)*	52%	855 (manual)/386 (remote control)

* NOTE: Because TSC is not reliability-based, the method results in a significantly different network capacity. The comparison here is that TSC provides a high capacity value which would increase EENS by 5000% considering manual LT and 2300% considering remote control LT.

Table 5
ELCC-Based Capacity Value (percentage load growth) for three different ESSs across three redundancy levels [16].

	2 MW/4 MWh	5 MW/10 MWh	10 MW/20 MWh
N-1	9.1%	14.8%	21.3%
N-0.75	6.1%	11.3%	17.3%
N-0.5	4.8%	10.0%	16.1%
ESS Cost (M€)	6.7	16.75	33.5

5. Discussion

5.1. Impact of base case reliability

Comparing the results of the different redundancy levels in Section 4.1 shows that the capacity value of LT depends on the base case EENS. LT provides more capacity contribution, when the initial reliability level is lower. A worse level of reliability means more frequent failures and more energy not supplied when a fault occurs. This, in turn, means that more demand (and more frequently) can be supplied via LT that would otherwise have been unserved.

5.2. Impact of a reliability level set by the network operator or the regulator

If an acceptable reliability level was determined by the DNO or the regulator, the maximum acceptable load growth would be different from the ELCC-based capacity value. For example, if the EENS index was set at 1 MWh/year in Section 4.1 (N-0.75 case), the load growth that would then be able to be accommodated is 25% of the base case demand (for manual LT). This is different to the ELCC-based capacity value of 14% that was calculated for this case. Consequently, the attitude of the DNO/regulator to risk could be a significant factor in the value that can be obtained from LT.

5.3. Regulatory implications

The findings of this study suggest the transition from a deterministic security of supply standard to a probabilistic or reliability-based one, which is also supported by the stochasticity of a number of smart grid assets, such as DG, DSR, ESSs, and RTTRs. The existing standard endeavors to define fixed values for stochastic quantities based on deterministic rules. An acceptable reliability index (e.g. EENS) can be determined by the utility or the regulator, which would then mean that a deterministic N-1 standard would not be required. The proposed approach can inform relevant standards, as well as the internal policies of DNOs.

5.4. Scalability

Reliability analysis using SMCS is computationally intensive, and embedding optimal load transfer within this framework increases the computational burden even further. A relaxed optimality gap can be used to enable the LT optimization to run within the SMCS; without this an optimal solution for a realistically sized DN can require a computational time ranging from half a minute to several minutes (see Section 4.2 and [22]). Moreover, the results show that the actual distance to optimality when using a relaxed optimality gap can be much lower than the MIPGap limit provided by the user. This enables high-quality solutions to be obtained in considerably less time than solving the model to optimality. This technique is also conservative in terms of reliability level: because the solution to the LT problem is sub-optimal, the EENS will be overestimated when using a relaxed optimality gap which will lead to a slight under-estimation of the ELCC. This is conservative, because the maximum allowable demand is guaranteed to be below the actual capability of the network (at the given reliability level).

5.5. Future work

In this paper LT has been considered as the only alternative to conventional network reinforcement. However, the value of LT may be affected by the addition of other smart interventions such as DSR or ESS; further work could therefore look at combinations of solutions, with DSR or ESS providing additional capacity headroom for LT, and LT enabling ESS or DSR to support multiple networks through interconnection. In addition, there are more advanced alternatives to the manual and remote control LT which have been considered here; future studies could investigate automation – including the challenges presented in the control scheme [45] – and replacing some switches with soft open points [1], power electronic devices (in place of conventional normally open points) which offer controllable active power flow between feeders and independent reactive power control at both AC terminal nodes. Furthermore, in all of the above cases it may be of interest to study the impact and scheduling of planned outages on the system's reliability by comparing seasons or specific types of day and adding scheduled outages to the random failures already included in the analysis.

As more and more distributed energy resources (DER) are installed in the low voltage system, there will be change in the demand seen in medium voltage (which is the voltage level considered in this paper). The results shown in the case study assumed that the demand would grow but the underlying demand patterns would remain the same. It could therefore be of value to use the method described in this paper in conjunction with models of future loading, including DER as well as uptake of low-carbon technologies such as electric vehicles and heat pumps, to study how future load patterns could affect the capacity value of LT.

6. Conclusion

This paper describes a new innovative probabilistic method to quantify the capacity value of LT using ELCC within a Sequential Monte Carlo Simulation framework (first contribution). This is a reliability-aware approach which – in contrast to the relevant literature – evaluates the change in reliability associated with increasing network loading and frames the decision in these terms. Optimal LT decisions, which determine the optimal LT when the network demand cannot be met by the available incoming circuit capacity, are carried out using a state-of-the-art MISOCP optimization formulation. The second contribution of this paper is the incorporation of the MISOCP problem into the SMCS using a relaxed optimality gap to provide high quality solutions in significantly less time than solving the model to global optimality, as well as the definition of the objective function to include network losses which improves load transfer performance by balancing load between feeders and ensures high quality of the convex relaxation of power flow equations.

The proposed methodology was demonstrated using a real-world distribution network operated by Taiwan Power Company for three redundancy levels: N-1, N-0.75, and N-0.5. According to this study, we can make the following concluding remarks:

- We obtained maximum capacity values of 25% and 37% of the base case demand for manual and remote-control LT, respectively, with an EENS of 4.21 MWh/year, which corresponds to the N-0.5 case.
- The capacity value of LT is significantly influenced by the redundancy level. The capacity values for the N-1 case (which corresponds to a base case EENS of 0.017 MWh/year) were just 7% and 16% for manual and remote control, respectively. These results indicate that the lower the acceptable base case EENS, the lower the capacity value of LT.
- Our method advances the state of the art by providing a reliability-based means by which DNOs can make better informed investment decisions, accommodating significant additional demand at a known and acceptable level of reliability.
- Finally, this work could inform relevant industry standards and utility internal policies.

CRediT authorship contribution statement

Ilias Sarantakos: Conceptualization, Data curation, Formal analysis, Investigation, Methodology, Resources, Software, Validation, Visualization, Writing - original draft. **David M. Greenwood:** Conceptualization, Data curation, Formal analysis, Funding acquisition, Investigation, Methodology, Project administration, Resources, Supervision, Visualization, Writing - review & editing. **Natalia-Maria Zografou-Barredo:** Formal analysis, Investigation, Methodology, Writing - review & editing. **Vahid Vahidinasab:** Writing - review & editing. **Phil C. Taylor:** Conceptualization, Funding acquisition, Supervision, Writing - review & editing.

Declaration of Competing Interest

The authors declare that they have no known competing financial interests or personal relationships that could have appeared to influence the work reported in this paper.

Acknowledgments

The first author would like to thank Mrs Antigone Mondelou for her valuable advice and support. This work was supported by the Engineering and Physical Sciences Research Council (EPSRC), UK (award reference 1645763), Siemens PLC, UK (reference 14220176), Northern Powergrid, UK as part of the Pragmatic Security Assessment NIA Project (NIA_NPG_029), and the EPSRC Supergen Energy Networks Hub (EP/S00078X/1). The authors would also like to thank seven anonymous reviewers for their valuable time to examine this paper.

References

[1] Romero-Ramos E, Gómez-Expósito A, Marano-Marcolini A, Maza-Ortega JM, Martinez-Ramos JI. Assessing the loadability of active distribution networks in the presence of DC controllable links. IET Gener Transm Distrib 2011;5(11):1105–13. https://doi.org/10.1049/iet-gtd.2011.0080.
[2] Strbac G, et al. Benefits of Advanced Smart Metering for Demand Response based Control of Distribution Networks, Report for the Energy Networks Association; 2010.
[3] Brown RE. Electric Power Distribution Reliability. New York: Marcel Dekker; 2002.
[4] Hegazy YG, Salama MMA, Chikhani AY. Adequacy assessment of distributed generation systems using Monte Carlo Simulation. IEEE Trans Power Syst 2003;18(1):48–52. https://doi.org/10.1109/TPWRS.2002.807044.
[5] Wang DTC, Ochoa LF, Harrison GP. DG impact on investment deferral: network planning and security of supply. IEEE Trans Power Syst 2010;25(2):1134–41. https://doi.org/10.1109/TPWRS.2009.2036361.
[6] Greenwood DM, Wade NS, Taylor PC, Papadopoulos P, Heyward N. A probabilistic method combining electrical energy storage and real-time thermal ratings to defer network reinforcement. IEEE Trans Sustain Energy 2017;8(1):374–84. https://doi.org/10.1109/TSTE.2016.2600320.
[7] Konstantelos I, Djapic P, Strbac G, Papadopoulos P, Laguna A. Contribution of

energy storage and demand-side response to security of distribution networks. CIRED - Open Access Proc J 2017;2017(1):1650–4. https://doi.org/10.1049/oap-cired.2017.0830.
[8] Energy Networks Association. Engineering Recommendation P2/7: Security of Supply; 2019.
[9] Henneaux P, Labeau P, Maun J, Haarla L. A two-level probabilistic risk assessment of cascading outages. IEEE Trans Power Syst 2016;31(3):2393–403. https://doi.org/10.1109/TPWRS.2015.2439214.
[10] ENTSO-E. Mid-term Adequacy Forecast 2019, Brussels, Belgium; 2019.
[11] Nolting L, Praktiknjo A. Can we phase-out all of them? Probabilistic assessments of security of electricity supply for the German case. Appl Energy 2020;263:114704https://doi.org/10.1016/j.apenergy.2020.114704.
[12] Méndez VH, et al. Impact of distributed generation on distribution investment deferral. Int J Elect Power Energy Syst 2006;28(4):244–52. https://doi.org/10.1016/j.ijepes.2005.11.016.
[13] Pudaruth GR, Li F. Locational Capacity Credit Evaluation. IEEE Trans Power Syst 2009;24(2):1072–9. https://doi.org/10.1109/TPWRS.2009.2016468.
[14] Dent CJ, Hernandez-Ortiz A, Blake SR, Miller D, Roberts D. Defining and evaluating the capacity value of distributed generation. IEEE Trans Power Syst 2015;30(5):2329–37. https://doi.org/10.1109/TPWRS.2014.2363142.
[15] Imperial College London. Review of Distribution Network Security Standards; 2015.
[16] Konstantelos I, Strbac G. Capacity value of energy storage in distribution networks. J Storage Mater 2018;18:389–401. https://doi.org/10.1016/j.est.2018.06.002.
[17] Xiao J, Li F, Gu WZ, Wang CS, Zhang P. Total supply capability and its extended indices for distribution systems: definition, model calculation and applications. IET Gener Transm Distrib 2011;5(8):869–76. https://doi.org/10.1049/iet-gtd.2010.0769.
[18] Xiao J, Li X, Gu W, Li F, Wang C. Model of distribution system total supply capability considering feeder and substation transformer contingencies. Int J Elect Power Energy Syst 2015;65:419–24. https://doi.org/10.1016/j.ijepes.2014.10.025.
[19] Chen K, Wu W, Zhang B, Djokic S, Harrison GP. A method to evaluate total supply capability of distribution systems considering network reconfiguration and daily load curves. IEEE Trans Power Syst 2016;31(3):2096–104. https://doi.org/10.1109/TPWRS.2015.2444792.
[20] Ding T, Li C, Zhao C, Wang M. Total supply capability considering distribution network reconfiguration under N - k transformer contingency and the decomposition method. IET Gener Transm Distrib 2017;11(5):1212–22. https://doi.org/10.1049/iet-gtd.2016.1071.
[21] Dorostkar-Ghamsari MR, Fotuhi-Firuzabad M, Safdarian A, Hoshyarzade AS, Lehtonen M. Improve capacity utilization of substation transformers via distribution network reconfiguration and load transfer. In: 2016 IEEE 16th International Conference on Environment and Electrical Engineering (EEEIC); 2016. p. 1–6, doi: 10.1109/EEEIC.2016.7555777.
[22] Jabr RA, Singh R, Pal BC. Minimum loss network reconfiguration using mixed-integer convex programming. IEEE Trans Power Syst 2012;27(2):1106–15. https://doi.org/10.1109/TPWRS.2011.2180406.
[23] Garver LL. Effective load carrying capability of generating units. IEEE Trans Power App Syst 1966; PAS-85 (8): 910–9, doi: 10.1109/TPAS.1966.291652.
[24] Amelin M. Comparison of capacity credit calculation methods for conventional power plants and wind power. IEEE Trans Power Syst 2009;24(2):685–91. https://doi.org/10.1109/TPWRS.2009.2016493.
[25] Zhou Y, Mancarella P, Mutale J. Framework for capacity credit assessment of electrical energy storage and demand response. IET Gener Transm Distrib 2016;10(9):2267–76. https://doi.org/10.1049/iet-gtd.2015.0458.
[26] Billinton R, Allan RN. Reliability evaluation of power systems. 2nd ed. New York: Plenum; 1996.
[27] Allan RN, Billinton R, Sjarief I, Goel L, So KS. A reliability test system for educational purposes – Basic distribution system data and results. IEEE Trans Power Syst 1991;6(2):813–20. https://doi.org/10.1109/59.76730.
[28] Billinton R, Li W. Reliability assessment of electric power systems using monte carlo methods. New York: Plenum; 1994.
[29] Energy Networks Association. Engineering Recommendation P27: Current rating guide for high voltage overhead lines operating in the UK distribution system; 1986.
[30] Jabr RA. Radial distribution load flow using conic programming. IEEE Trans Power Syst 2006;21(3):1458–9. https://doi.org/10.1109/TPWRS.2006.879234.
[31] Gurobi Optimization LLC. Gurobi Optimizer Reference Manual. http://www.gurobi.com.
[32] IBM. IBM ILOG CPLEX Optimization Studio. www.cplex.com.
[33] MOSEK ApS. The MOSEK Optimization Tools Version 9.0. http://www.mosek.com/.
[34] Gurobi Optimization LLC. Mixed-Integer Programming (MIP) – A Primer on the Basics. https://www.gurobi.com/resource/mip-basics/.
[35] Su C-T, Lee C-S. Network reconfiguration of distribution systems using improved mixed-integer hybrid differential evolution. IEEE Trans Power Del 2003;18(3):1022–7. https://doi.org/10.1109/TPWRD.2003.813641.
[36] Sarantakos I, Greenwood DM, Yi J, Blake SR, Taylor PC. A method to include component condition and substation reliability into distribution system reconfiguration. Int J Elect Power Energy Syst 2019;109:122–38. https://doi.org/10.1016/j.ijepes.2019.01.040.
[37] Statutory Instruments. The Electricity Safety, Quality and Continuity Regulations 2002, No. 2665; 2002.
[38] National Grid. Current Ratings for Overhead Lines; 2001.
[39] Greenwood D, Wade N, Heyward N, Mehta P, Taylor P, Papadopoulos P. Scheduling power and energy resources on the smarter network storage project. In: 23rd Int. Conf. Exhibition on Electricity Distribution (CIRED), Lyon, France; 2015.
[40] Sarantakos I. Investigating the Impact of Asset Condition on Distribution Network Reconfiguration and its Capacity Value PhD Thesis UK: Newcastle University; 2019.
[41] Information from Northern Powergrid DNO, UK; 2020.
[42] Saboori H, Hemmati R, Ghiasi SMS, Dehghan S. Energy storage planning in electric power distribution networks – A state-of-the-art review. Renew Sustain Energy Rev 2017;79:1108–21. https://doi.org/10.1016/j.rser.2017.05.171.
[43] Bouhouras AS, Andreou GT, Labridis DP, Bakirtzis AG. selective automation upgrade in distribution networks towards a smarter grid. IEEE Trans Smart Grid 2010;1(3):278–85. https://doi.org/10.1109/TSG.2010.2080294.
[44] Greenwood DM, Lim KY, Patsios C, Lyons PF, Lim YS, Taylor PC. Frequency response services designed for energy storage. Appl Energy 2017;203:115–27. https://doi.org/10.1016/j.apenergy.2017.06.046.
[45] Radhika C, Bharathan PK. Automatic load transfer in electrical power system (In ring electrical network). In: 2015 International Conference on Power, Instrumentation, Control and Computing (PICC); 2015. p. 1–8, doi: 10.1109/PICC.2015.7455766.